

Article

Approaching a Zero-Waste Strategy in Rapeseed (*Brassica napus*) Exploitation: Sustainably Approaching Bio-Based Polyethylene Composites

Roberto Aguado ¹, Francesc Xavier Espinach ¹, Fabiola Vilaseca ², Quim Tarrés ^{1,3,*}, Pere Mutjé ¹ and Marc Delgado-Aguilar ¹

¹ LEPAMAP-PRODIS Research Group, University of Girona, Maria Aurèlia Capmany 61, 17003 Girona, Spain; roberto.aguado@udg.edu (R.A.); francisco.espinach@udg.edu (F.X.E.); pere.mutje@udg.edu (P.M.); m.delgado@udg.edu (M.D.-A.)

² Advanced Biomaterials and Nanotechnology, Department of Chemical Engineering, University of Girona, Maria Aurèlia Capmany 61, 17003 Girona, Spain; fabiola.vilaseca@udg.edu

³ Chair on Sustainable Industrial Processes, University of Girona, Maria Aurèlia Capmany 61, 17003 Girona, Spain

* Correspondence: joaquimagusti.tarres@udg.edu

Abstract: The current need to develop more sustainable processes and products requires the study of new materials. In the field of plastic materials, the need to develop 100% bio-based materials that meet market requirements is evident. In this sense, the present work aims to explore the potential of rapeseed waste as a reinforcement of a bio-based plastic matrix that does not generate new sub-waste. For this purpose, three types of processing of rapeseed residues have been studied: (i) milling; (ii) mechanical process; (iii) thermomechanical process. In addition, the reinforcing capacity of these materials, together with the need for an optimized coupling agent at 6 wt.%, has been verified. The micromechanics of the materials have been evaluated to determine the development of these fibers in the composite material. The results obtained show remarkable increases in mechanical properties, reaching more than 141% in tensile strength and 128% in flexural strength. There is a remarkable difference in the impact behavior between the materials with milled rapeseed and the fibers obtained by mechanical or thermomechanical processes. It was found that by sustainable design it is possible to achieve a 76.2% reduction in the amount of plastic used to manufacture material with the same mechanical properties.

Keywords: biocomposites; mechanical properties; micromechanical; sustainable design; zero-waste; rapeseed residue



Citation: Aguado, R.; Espinach, F.X.; Vilaseca, F.; Tarrés, Q.; Mutjé, P.; Delgado-Aguilar, M. Approaching a Zero-Waste Strategy in Rapeseed (*Brassica napus*) Exploitation: Sustainably Approaching Bio-Based Polyethylene Composites. *Sustainability* **2022**, *14*, 7942. <https://doi.org/10.3390/su14137942>

Academic Editor: Paris Fokaides

Received: 3 June 2022

Accepted: 25 June 2022

Published: 29 June 2022

Publisher's Note: MDPI stays neutral with regard to jurisdictional claims in published maps and institutional affiliations.



Copyright: © 2022 by the authors. Licensee MDPI, Basel, Switzerland. This article is an open access article distributed under the terms and conditions of the Creative Commons Attribution (CC BY) license (<https://creativecommons.org/licenses/by/4.0/>).

1. Introduction

The use of plastic materials for the production of a multitude of products for daily use has become a topic of great controversy. New regulations regarding the use of plastic in single-use products have generated enormous concern about the future of plastic [1,2]. The great properties offered by plastics in their use in semi-structural applications are difficult to achieve with other materials, which is why new alternatives must be developed. It seems clear that the plastics of the future must be renewable in origin and, if possible, biodegradable [3,4]. However, several limitations must be considered. First, the current price of these materials. Currently, plastics such as polylactic acid (PLA), one of the most promising, cost approximately 1.7 times more than polypropylene or polyethylene [5]. Second the properties that these new plastics can offer. Economically viable plastics, such as thermoplastic polystyrene (TPS), have properties far removed from those of current plastics. For example, in terms of tensile strength, TPS has a value of 3–5 MPa compared to 16–20 MPa for HDPE [6–9]. Third, the large-scale availability of these bioplastics. There

are still few plastics of natural and bio-based origin that are at a level of industrialization sufficient for immediate market incorporation [10,11]. Fourth, the conditions of use to which they will be subjected. Plastics with a high biodegradation rate can hardly be used in outdoor applications. Finally, the difficulties of recycling these bioplastics. One of the main problems with the use of plastics such as PLA is the lack of a recycling stream for these materials. Therefore, the development of materials based on bio-based plastics that are chemically the same as fossil-based plastics, such as bio-polyethylene, can be a great alternative.

Renewable polyethylene (BioPE) is produced mainly from sugar cane [10]. It is chemically identical to polyethylene and can be found on an industrial scale. However, its price today is still higher than that of polyethylene of fossil origin [11]. Hence, new methods must be sought to develop materials using the minimum amount of this polymer and to increase the sustainability of the final products. One of the areas being explored by many researchers is the production of composite materials with natural fibers. The incorporation of natural fibers has great advantages, such as obtaining considerable improvements in mechanical properties, the replacement of part of the polymer with a renewable and biodegradable resource, etc. [12–14]. However, there are also some challenges to overcome. First, the poor compatibility between a material with a hydrophilic character (natural fibers) and a hydrophobic material (plastic polymers) [15]. Second, the modification of the material's density by incorporating a denser component such as natural fibers. Third, the restrictions of processing temperatures to values that do not exceed 220 °C [16]. Fourth, the origin and sustainability of the processes used to obtain these fibers. In addition, replacing commonly used synthetic fibers such as fiberglass with natural fibers can reduce the contamination associated with these materials [17]. The use of agricultural residues represents a great opportunity in this sense since it is possible to obtain a renewable and biodegradable reinforcement by adding value to a residue that would otherwise be burned, generating CO₂ emissions [18].

Currently, rapeseed production is the third most important oilseed worldwide. Mainly, interest is focused on the oil (40% of its content) [19]. However, its production, as in the case of other food crops, generates a large amount of residues in the form of straw. This factor, together with the prediction of a significant increase in worldwide demand for edible oilseed products, presents the residues of this crop as an important source of cellulosic resources [20]. Moreover, its use could not only add value to a waste product, but also increase economic activity in rural regions.

On the other hand, the use of zero-waste generation methodologies must be considered in comparison to the classical fiber production methodologies used by the pulp and paper industry. It is well known that kraft, sulfite, etc. pulping methods and bleaching technologies involve the use of a large number of chemical reagents and the generation of waste [21]. Therefore, if we want to improve the sustainability of these materials, the principles of green chemistry must be applied. Hence, this work is perfectly aligned with the first and seventh principles of green chemistry [22].

This work aims to obtain fully bio-based composite materials reinforced with rapeseed residue through a zero waste process. For this purpose, it focuses on the use of rapeseed residue processed through three different methodologies that do not generate residues: milling, mechanical process, and thermomechanical process. The reinforcing capacity of these three types of rapeseed fibers on a bio-polyethylene matrix with fiber content between 20 and 50 wt.% has been evaluated. The need for a coupling agent has been found and optimized, and the micromechanics of the composites have been studied. Furthermore, we demonstrate and confirm that the use of these natural fibers from agricultural waste allows us to decrease the amount of plastic polymer used by counteracting the effect of the increase in the density of the material. Therefore, the present study presents a clear option for the substitution of fossil-based plastic materials in semi-structural applications. The article presents a novel way to valorize rapeseed residues without generating waste.

Obtaining completely bio-based reinforced materials and the study of this reinforcement in the density of the material allows the development of more sustainable materials.

2. Materials and Methods

Bio-polyethylene (BioPE) from sugarcane was purchased from Braskem (Sao Paulo, Brazil). The grade of BioPE used was an injection molding grade SHA7260 with a density of 0.955 g/cm^3 and a melt flow rate of $20 \text{ g}/10 \text{ min}$. Anhydride maleic grafted polypropylene (MAPE) was used as a coupling agent in a moderate amount. MAPE was obtained from Eastman Chemical Products (San Roque, Spain) under the commercial name Fusabond MB100 D with a density of 0.960 g/cm^3 and a melt flow rate of $2.0 \text{ g}/10 \text{ min}$. The level of anhydride maleic grafted polypropylene was over 1 wt.%. Rapeseed (*Brassica napus*) waste was used as a raw material for extraction of natural fibers. Rapeseed waste was supplied by Mas Clara S.L. (Domeny, Spain) as a stalk obtained after the harvest.

2.1. Compound Generation

The flowchart of the applied method is shown in Figure 1. This blueprint starts with the rapeseed stalk waste processing followed by the compound generation and the test specimen's production and characterization.

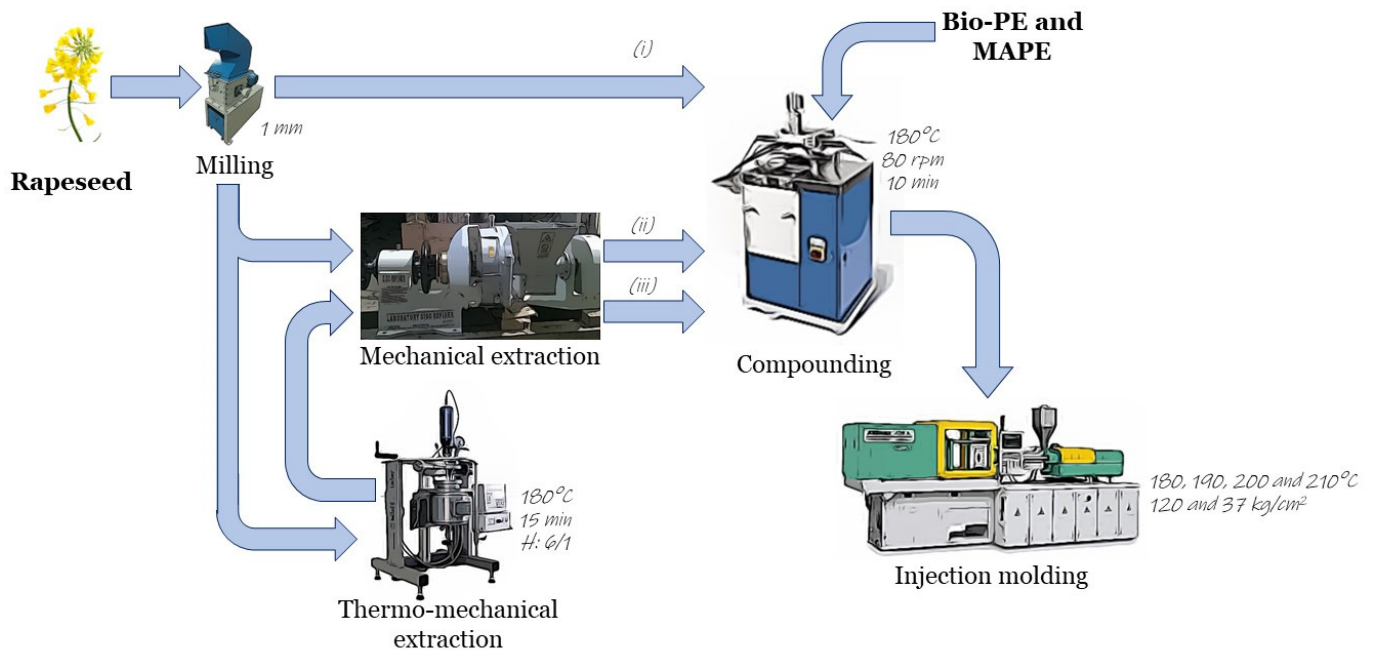


Figure 1. Scheme of process methodology.

Natural fibers from rapeseed waste were obtained using three different methodologies: (i) milling; (ii) mechanical extraction; and (iii) thermomechanical extraction.

Milling: rapeseed stalks including nodes were received and ground in a miller Agrimsa (Agrimsa, St. Adrià del Besós, Spain) into small pieces before screening with a 1 mm size hole screen.

Mechanical extraction: rapeseed after the screening was passed through Sprout–Waldron equipment (Andritz, Spain) using water as a medium for defibrillation.

Thermomechanical extraction: rapeseed particles were digested using steam–water at $180 \text{ }^\circ\text{C}$ for 15 min with a liquid ratio kept at six parts of water for each part of the dry weight of rapeseed using a pressure reactor. Digested fibers were washed and passed through Sprout–Waldron equipment.

Then, the obtained rapeseed fibers were dried at $80 \text{ }^\circ\text{C}$ for at least 48 h before use in an oven Dycometal AFA288 (Dycometal Inc., Viladecans, Spain) before use.

Compounding was carried out by the mixing of BioPE and rapeseed fibers in a Brabender W 50 EHT (Brabender GmbH & Co. KG, Duisburg, Germany). The equipment was heated to 180 °C before BioPE (was introduced. Then, BioPE (50–100 wt.%) was melted together with MAPE (0–8 wt.%) at 80 rpm. Finally, rapeseed fibers (0–50 wt.%) were introduced and mixed for 10 min. The resulting material was pelletized with a knife mill (Retsch Cutting Mill SM-100, Retsch GmbH, Haan, Germany) and dried at 80 °C until it was used in injection molding. It is important to note that percentage coupling agent is calculated from the weight of the rapeseed content and not from the whole weight of the composite.

Standard specimens, of 115 mm length with narrow grips, 13 mm gage width, and 3.2 mm thickness (ASTM D638-14), were fabricated by an injection-molding machine (Arburg 220M 350-90U, Arburg, Lossburg, Germany). The temperature profile used during the injection molding process was 180, 190, 200, and 210 °C. The first and second pressures were 120 kg/cm² and 37.5 kg/cm², respectively. Standard specimens were kept in a climatic chamber (Dycometal CCK-30/1000, Dycometal Inc, Viladecans, Spain) at 23 °C and 50% relative humidity for at least 48 h before characterization (ASTM D618).

2.2. Composite Characterization

The chemical composition of obtained fibers was determined in terms of ash, lignin, pentosans, and cellulose content. Ash content was determined according to TAPPI T211 by gravimetric analysis of the sample ignited in a muffle furnace at 525 °C. Acid-insoluble lignin was determined over a free-extractives sample by acid hydrolysis according to TAPPI T222. Pentosan content was colorimetrically determined after acid boiling according to T223. Finally, cellulose content was estimated as the difference from the analyzed compounds.

Composite materials were characterized in terms of tensile, flexural, and impact tests, physical properties, microscopic examination, and fiber morphology analysis.

Tensile and flexural tests were performed in a Hounsfield H2.5K-S universal test machine (Redhill, UK). Tensile strength, Young's modulus, and elongation at break were studied by means of tensile tests. For the tensile test, Tinius Olsen PS50C 0226 extensometer (Redhill, UK) was used to calculate Young's modulus. Tensile tests were conducted according to the standard ASTM D638 and the tensile speed was 5 mm/min. Flexural tests were performed with three-point bending method according to ASTM D790 standard, with a 2 mm/min test speed and 52 mm length between supports.

The dynamic property (impact tests) of composite materials was measured by Ceast impact apparatus (Norwood, MA, USA) and Charpy hammer was used. The 2.75 J hammer broke the samples notched and unnotched with a 3.45 m/s test speed, according to ISO 179-1-2000. To obtain notched samples a Ceast NotchVis equipment (Norwood, MA, USA) was used.

The melt flow rate of composites was measured by a Ceast flow meter (Norwood, MA, USA) at 210 °C with a 10 kg load for 10 min. The capillary with a 9 mm total diameter and 2 mm hole diameter was used. The density of the composite materials was measured with a pycnometer and calculated using the following equation:

$$\rho_C = \frac{m_2 - m_1}{(m_4 - m_1) - (m_3 - m_2)} = \frac{m_C}{V_C} \quad (1)$$

where ρ_C is the density of the composite (g/cm³), m_1 is the weight of the pycnometer (g), m_2 is the weight of the pycnometer with a composite piece (g), m_3 is the weight of the pycnometer with distillate water (g), m_4 is the weight of the pycnometer with the composite piece refilled with distillate water (g), m_C is the weight of the composite (g), and V_C is the volume of the composite (cm³).

Fiber and matrix adhesion was examined using a Zeiss DSM 960 A scanning electron microscope with 20 kV electron beam to achieve 5000-fold magnification. To obtain adequate fracture, specimens had been previously frozen in liquid nitrogen. Silver and gold surface treatments were used.

Fiber morphology after each treatment and extracted from the composite was analyzed in a Morfi fiber analyzer (Techpap, Gières, France). Fiber composite extraction was carried out in a Soxhlet apparatus using decalin as the solvent. After at least 24 h of extraction, the fibers were rinsed with acetone and distilled water. Morphological analysis was used to obtain fiber distribution, arithmetic length (l_a^F), weight-weighted length (l_w^F), and average fiber diameter (d^F).

The evaluation of the micromechanical properties was carried out in terms of the efficiency factor (f_c), interfacial tension (τ), critical length (L_c^F), intrinsic strength of the fibers (σ_t^F), orientation factor (χ_1), length factor (χ_2), and the average orientation angle (α).

3. Results

3.1. Rapeseed Fibers Analysis

The fiber extraction by three different methodologies is designed to obtain a zero-waste strategy. In Table 1, the yield of fiber extraction, chemical composition, and morphology analysis for each procedure is presented.

Table 1. Chemical composition and morphological analysis of the rapeseed fibers.

Fiber	Yield (%)	Chemical Composition				Morphology			
		Cellulose ¹ (%)	Lignin (%)	Pentosans (%)	Ash (%)	Length (μm)	Width (μm)	Fines (%)	Aspect Ratio ²
Milled rapeseed (MR)	99.7 ± 0.2	50.6	19.8 ± 1.7	23.8 ± 1.6	5.8 ± 0.4	1354 ± 78	31.7 ± 0.2	8.0 ± 2.4	42.7
Mechanical rapeseed fibers (MRF)	98.1 ± 0.4	51.7	19.3 ± 1.5	24.1 ± 1.8	4.9 ± 0.6	412 ± 22	22.4 ± 0.1	46.7 ± 7.8	18.4
Thermomechanical rapeseed fibers (TMRF)	95.3 ± 0.3	53.4	17.3 ± 1.1	26.6 ± 1.4	2.7 ± 0.5	528 ± 23	22.0 ± 0.2	37.2 ± 8.3	24.0

¹ Calculated as the difference to the rest of the components. ² Calculated as fiber length (l^F) divided by fiber width (d^F).

As expected, milling and mechanical extraction of rapeseed fibers do not involve any material removal. Hence, the slow diminution in the yield is related to mass lost during the processing. However, the reduction in the yield of the thermomechanical process is also a result of water-soluble component extraction [23]. The yield of rapeseed fibers obtained from raw material was over 95% in the three cases. Therefore, it might be concluded that the three methodologies allow integral exploitation of this residue. These results were consistent in chemical composition analysis. There were no significant differences in the chemical composition of milled rapeseed (MR) and mechanical rapeseed fibers (MRF). Meanwhile, thermomechanical rapeseed fibers (TMRF) showed a slight decrease in ash and lignin content. Milled rapeseed results in large particle sizes containing large fiber bundles. The mechanical extraction process involves the crushing and grinding of rapeseed stalks using rotating metal discs. This refining method involves an important length reduction from 1354 μm to 412 μm . In the same sense, the diameter of the fibers is drastically reduced from 31.7 μm to 22.4 μm . This phenomenon is a result of the random mechanical breakage of rapeseed to obtain fiber separation [24]. However, this unselective process also leads to a significant increase in the fines content, which is 5.8 times higher than that of milled rapeseed (from 8.0 to 46.7%). In contrast, thermomechanical extraction entails lignin softening and enhances fiber separation [25]. In this sense, fiber length was slightly reduced in comparison to MRF (from 1354 μm to 528 μm). However, the fiber width decreased from 31.7 μm to 22.0 μm . This results in an increased aspect ratio of TMRF. In addition, the greater selectivity of this additional step during fiber extraction implies a slow increase in fines content.

3.2. Coupling Agent Dosage Study

Before the studies of the main composites, a sufficient amount of the coupling agent for each treated fiber was assessed. Previous studies have shown that adding the coupling agent as a function of the amount of reinforcement did not change the interface strength [26–28]. This can be explained by the relationship of sites ready for coupling and

adhesion in natural fibers (Figure 2a). Therefore only the composition of 30 wt.% fibers was tested with different percentages of coupling agent (Figure 2b).

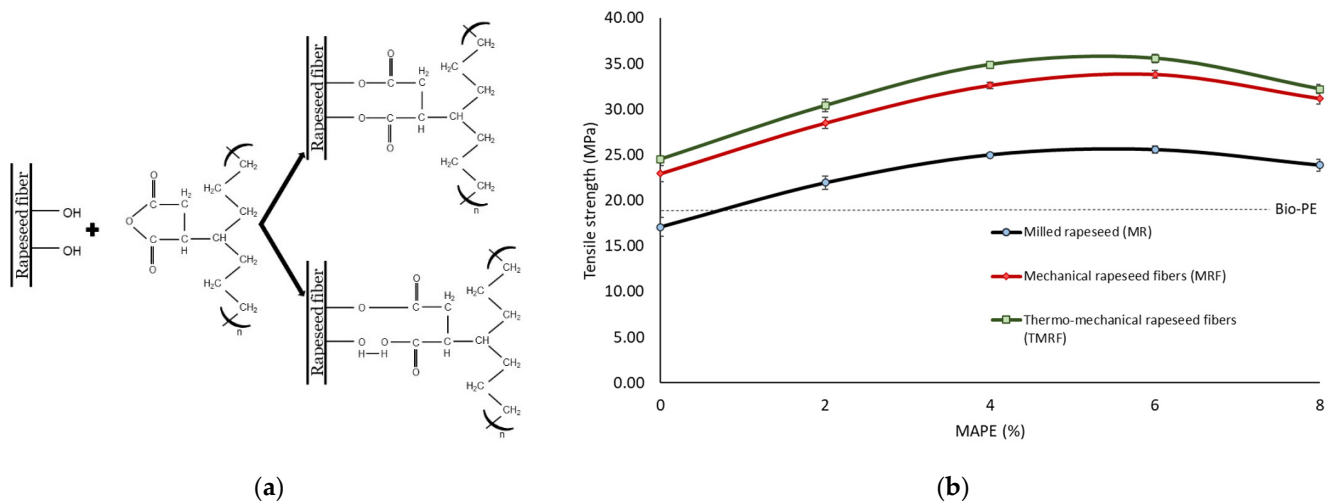


Figure 2. (a) Interaction mechanism between rapeseed fibers and coupling agent (MAPE); (b) effect of coupling agent on tensile strength in 30 wt.% rapeseed reinforced BioPE composites.

As is shown in Figure 2a, the chemical interaction between the hydroxyl group of the rapeseed fiber and the functional groups of maleic anhydride affects the morphology of the polymer composition [29]. By focusing on the trends in the tensile strength–MAPE content diagram, it can be ascertained that the usage of a coupling agent is necessary, otherwise milled rapeseed (MR) acts as a filler and not as a reinforcement, and mechanical rapeseed fibers (MRF) and thermomechanical rapeseed fibers (TMRF) do not fully develop their reinforcement potential. Scanning electron microscope (SEM) images show the effect of the coupling agent on the fiber–matrix adhesion (Figure 3).

It can be observed that the composite without a coupling agent presents more errors in the strength transfer between the rapeseed fibers and the BioPE (Figure 3a,b). Fibers inside the composites without a coupling agent were pulled out and left holes in the matrix material. The strong adhesion promoted by MAPE improves the strength transfer to the fibers until broken. Another kind of failure is the fibers delaminating when the fiber has eligible adhesion, but the orientation is normal to the strain as shown in Figure 3a. Figure 3c,d shows the adhesion of one fiber on 30 wt.% thermomechanical rapeseed fibers reinforced composite with and without coupling agent. In the case without coupling agent, a gap between fiber and matrix is found. The gap can be caused by the thermal shrinkage of the BioPE, which means a weak fiber–matrix interaction.

In sight of the increasing growth of the tensile strength, 6% coupling agent is the most appropriate amount. The addition of higher than 6% coupling agent contents drives a decrease in the tensile strength of the composite. This phenomenon is related to the lower molecular weight of MAPE polyethylene chain than BioPE and the interface fiber–matrix saturation (MAPE not bonded to rapeseed fibers) [28]. On the other hand, a clear difference can be seen between the results obtained in the case of milled rapeseed (MR) and those of the fibers extracted by mechanical and thermomechanical processes (MRF and TMRF). This is explained by the large difference in diameter, with milled rapeseed being closer to chips than to fibers.

On the other hand, the results obtained for the Young’s modulus at different coupling agent percentages allow us to observe two phenomena (Figure 4). First, there is no influence between the quality of the interface and the young’s modulus, as previously reported. Second, the higher stiffening of the material by the extracted fibers. This is due to the higher intrinsic stiffness of the smaller diameter fibers.

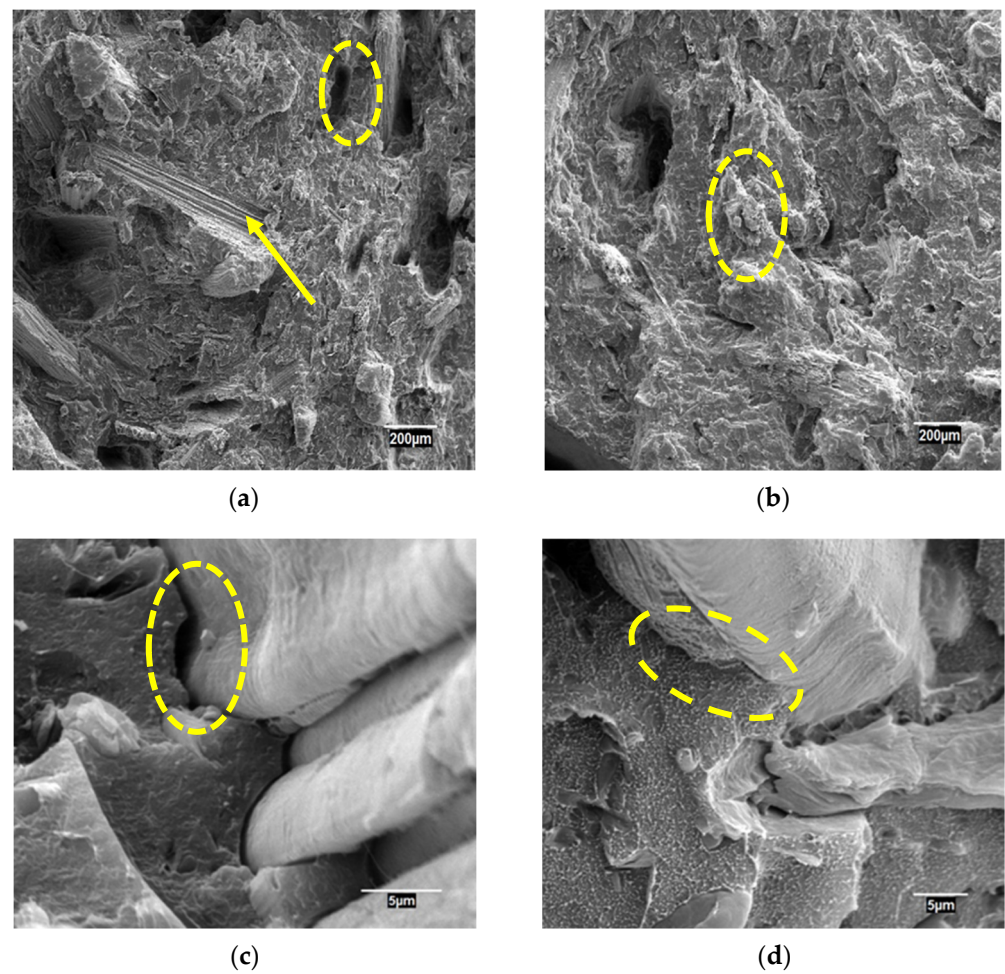


Figure 3. Scanning electron microscopy (SEM) images of 30 wt.% TMRF composite: (a,c) without coupling agent; (b,d) with 6% coupling agent. Details in yellow circles and arrow.

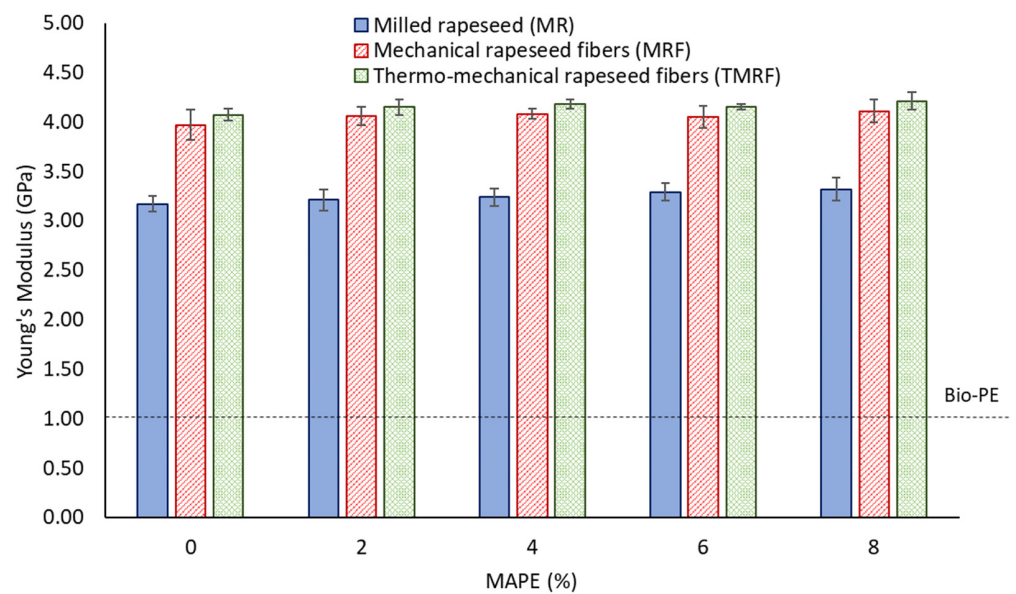


Figure 4. Effect of coupling agent on Young's modulus in 30 wt.% rapeseed reinforced BioPE composites.

In view of the coupling agent dosage study, the 6% coupling agent is enough for technical reasons and it will be eligible for further analysis.

3.3. Physical Properties of Composites

The incorporation of a material with a higher density than that of the plastic matrix leads to an increase in the final density of the composite material. Thus, a greater reinforcement of the material will also lead to heavier material. It is therefore important to consider not only the increase in mechanical properties that such reinforcement can provide but also how it modifies its physical properties. As shown in Table 2, for a reinforcement content of 20 wt.% the density of the composite increases from 0.955 g/cm³ (BioPE density) to 1.002 g/cm³ for milled rapeseed (MR) and to 1.004 and 1.005 g/cm³ for MRF and TMRF fibers, respectively. These results indicate, as expected, a higher density of the fibers with higher treatment. Considering the weight of the specimen, the density of the composite, and the density of the BioPE, it can be estimated that the density of the different reinforcements studied is 1.32, 1.36, and 1.38 g/cm³ for MR, MRF, and TMRF, respectively. The densities obtained are similar to those reported in the literature for fibers from agricultural residues [30].

Table 2. Physical properties of composites and morphological analysis of extracted fibers.

Fiber	Content (wt.%)	Density (g/cm ³)	V ^F	l _a ^F (μm)	l _w ^F (μm)	Width (μm)	Aspect Ratio ¹
MR	20	1.002 ± 0.005	0.154	303.82 ± 8.33	707.82 ± 7.42	29.6 ± 0.2	10.26
	30	1.027 ± 0.001	0.238	293.51 ± 11.24	686.64 ± 9.56	29.3 ± 0.1	10.02
	40	1.054 ± 0.009	0.327	280.44 ± 14.33	642.70 ± 11.21	29.2 ± 0.1	9.60
	50	1.085 ± 0.003	0.421	268.19 ± 9.42	598.08 ± 8.16	28.9 ± 0.2	9.28
MRF	20	1.004 ± 0.002	0.150	280.60 ± 15.64	599.94 ± 12.21	20.7 ± 0.1	13.56
	30	1.030 ± 0.007	0.232	251.09 ± 8.21	556.16 ± 7.45	20.1 ± 0.2	12.49
	40	1.060 ± 0.004	0.320	232.16 ± 9.74	487.34 ± 8.76	19.7 ± 0.2	11.78
	50	1.093 ± 0.008	0.414	219.91 ± 16.21	463.77 ± 13.42	19.5 ± 0.1	11.28
TMRF	20	1.005 ± 0.001	0.148	323.24 ± 7.94	724.34 ± 6.37	19.9 ± 0.1	16.24
	30	1.032 ± 0.007	0.230	305.84 ± 5.11	710.14 ± 5.88	19.7 ± 0.1	15.52
	40	1.062 ± 0.006	0.317	291.63 ± 6.89	661.35 ± 6.91	19.4 ± 0.2	15.03
	50	1.097 ± 0.009	0.410	275.60 ± 8.36	606.68 ± 7.77	19.3 ± 0.1	14.27

¹ Calculated as fiber length (l_a^F) divided by fiber width (d^F).

On the other hand, as mentioned above, in all three cases the density of the composite increases as the reinforcement content increases, reaching in the highest case (50 wt.% TMRF) a density of 1.097 g/cm³. By way of example, the manufacture of a single piece 10 cm high, 10 cm wide, and 0.5 cm thick would weigh 47.75 g if manufactured with BioPE. On the other hand, if this piece is manufactured with 30 wt.% reinforcement, it would weigh 51.35, 51.50, and 51.60 g for the composites with MR, MRF, and TMRF, respectively. This means an increase in weight of 7.54, 7.85, and 8.06% respectively.

Although usually weight percentages were used for the preparation of composite materials, the determination of the volume fraction occupied by the fibers used as reinforcement is necessary for a correct evaluation of the mechanical properties. The higher the density of the fiber for the same percentage by weight, the lower the volume fraction will be. In the same way, when the percentage by weight of the same fiber increases, the volume fraction increases. If the results of Table 2 are observed, the highest volume fraction of fibers used was for the composite with 50 wt.% of MR and the lowest volume fraction was for the composite with 20 wt.% of TMRF.

Table 2 also presents the morphological results of the fibers extracted for each of the different composites obtained. Two important phenomena are observed in this case. First, we can observe a significant reduction in fiber length, very important in the case of milled rapeseed (MR), from the original 1354 μm to 303.82 μm of the fibers extracted

in the composite with 20 wt.%; this is a 77.6% reduction in length. However, the fiber diameter was not greatly affected by the compounding plus injection process (from 31.7 μm to 29.6 μm). On the other hand, the mechanically and thermomechanically extracted fibers show a smaller reduction in fiber length of 31.9 and 38.8% for the MRF and TMRF fibers, respectively. In this case, both fibers present a slight reduction in diameter after being subjected to the whole process of obtaining the composite material. This decrease in fiber length and diameter can be explained due to the shear forces that these fibers experience when impacting the screw and the walls of the compounding chamber, as well as the pressure to which they are subjected during the injection process [31]. Second, it is also observed that the reduction in length and diameter increases with increasing fiber content, of 11.7, 21.6, and 14.7% when going from 20 to 50 wt.% for MR, MRF, and TMRF fibers. This can be explained by the shear forces experienced between the fibers themselves during processing, with a higher probability of collision when a greater number of fibers were present.

The results of the morphological analysis of the extracted fibers also show that the higher the treatment for the extraction of the fibers, the higher the aspect ratio obtained for the same percentage of reinforcement. This already indicates that TMRF fibers have a higher reinforcement potential than MR fibers. However, this aspect ratio is reduced with increasing fiber content, as a consequence of the greater reduction in fiber length as indicated above.

The rheological properties of thermoplastic polymers are extremely important during manufacturing. A low-viscosity material could improve the throughput, especially in the case of injection molding and extrusion. However, fibers in a composite always increase the viscosity and render a more difficult and slower manufacturing process. To examine the effect of the increased fiber content on the rheological properties the melt flow rate (MFR) test was applied. However, this method is not suitable for comparing the composites with the pure matrix material since the differences are of orders of magnitude. The results of these tests are shown in Figure 5.

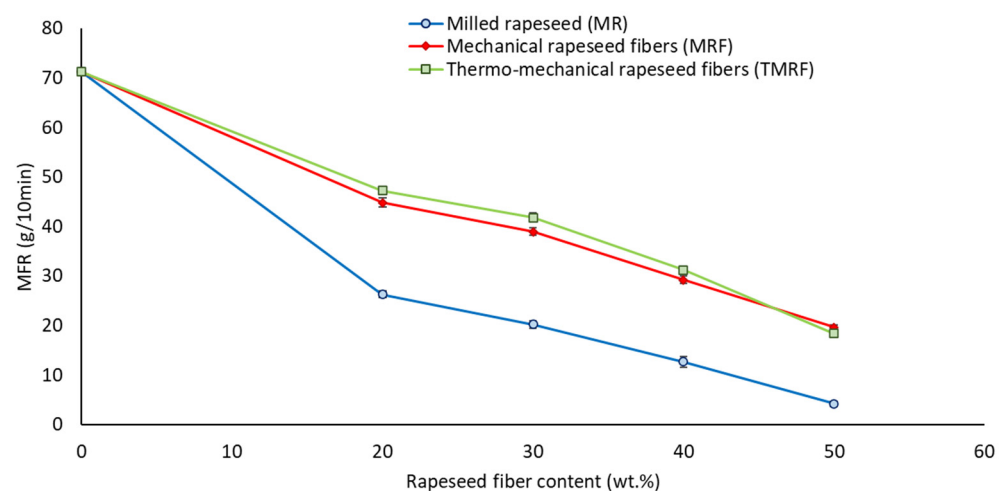


Figure 5. MFR of the different rapeseed-reinforced composites with 6% coupling agent.

The trend shown in this diagram is a decrease with increasing fiber content, especially in the case of milled rapeseed. Bio-polyethylene, which is originally a low-viscosity product, causes an important reduction in melt flow rate with fibers. In addition, the increasing fiber content increases the fiber damage and decreases the flowability of the melt. It is observed that the fibers obtained by mechanical (MRF) and thermomechanical (TMRF) treatment present very similar melt flow rate values for the different fiber contents tested. However, these values are significantly higher than those of milled rapeseed. This may be due to the larger size of the MR, as previously reported [32]. On the other hand, practically linear behavior is observed for the three types of fibers, resulting in predictable melt flow

rate behavior at different fiber contents. This linear behavior also indicates the correct processing of the material, with a correct distribution of the fibers in it. It should be noted that low melt flow rate values lead to greater difficulty in processing the material by injection, requiring higher pressures and/or temperatures. For this reason, it does not work with higher fiber contents.

3.4. Composite Macromechanical Analysis

The results obtained from the mechanical characterization of the composites with coupling agent for the different fibers studied with contents between 20 and 50 wt.% are presented below.

In Table 3, it can be seen how, in all cases, the incorporation of fibers with 6% MAPE leads to an increase in tensile strength. However, if we compare the three fibers we can see how, as mentioned above, the reinforcing capacity of the TMRF is superior. It can be seen that the increase in the reinforcement content leads to a higher tensile strength, with 88.6, 134.7, and 141.6% increase for a 50 wt.% reinforcement by MR, MRF, and TMRF, respectively. In addition, a linear trend is observed between the tensile strength and fiber content in all three cases. This leads to the expectation of a strong fiber–matrix interface, which would indicate that the observed differences in tensile strength are due to the intrinsic strength of the fibers [33]. If the values obtained are compared with published results for similar fibers such as wheat straw, rice straw, and other agricultural residues without coupling agents, it can be observed that superior results have been obtained in terms of increases in tensile strength, which confirms the strong interface obtained [34–36]. In this sense, if the results obtained are compared with those presented for sugarcane bagasse fibers with a coupling agent, it can be observed that the maximum increase obtained is 61.78%, lower than that of rapeseed fibers [37]. On the other hand, as expected, the reinforcing capacity of fibers from rapeseed is lower than that of synthetic fibers such as glass fibers, which causes much higher increases in tensile strength [38]. This will be further confirmed by micromechanical analysis of the tensile strength. When examining Young’s modulus results, the linear ratio is also visible between the reinforcement content and Young’s modulus for each fiber. However, in this case, the increasing rapeseed fiber percentage increases the results for all specimens, even if they are without a coupling agent, as previously mentioned. With the presence of the fibers, the samples become stiffer as the reinforcement content is increased, although there is no reasonable adhesion between the fibers and the thermoplastics. The increase in Young’s modulus values should be noted as well: the BioPE with 50 wt.% TMR is 5.9 times stiffer than their matrix material. This means there is no way to produce flexible parts with a high content of rapeseed fibers without other additives. These results are in agreement with the literature, which evidences the strong impact of natural fibers on Young’s modulus [28,39,40].

Table 3. Mechanical properties of composite materials of BioPE and rapeseed with 6% MAPE.

Fiber	Content (wt.%)	Tensile Properties			Flexural Properties			Impact Properties	
		Tensile Strength (MPa)	Young’s Modulus (GPa)	Elongation at Break (%)	Flexural Strength (MPa)	Flexural Modulus (GPa)	Deformation (mm)	Charpy Unnotched (kJ/m ²)	Charpy Notched (kJ/m ²)
-	0	18.12 ± 0.32	1.04 ± 0.02	12.23 ± 0.67	21.25 ± 0.24	0.84 ± 0.03	9.80 ± 0.12	Not break	7.57 ± 0.09
MR	20	22.13 ± 0.17	2.06 ± 0.03	3.31 ± 0.32	26.34 ± 0.38	1.28 ± 0.07	6.66 ± 0.22	12.09 ± 0.18	4.73 ± 0.02
	30	25.57 ± 0.29	3.29 ± 0.05	1.24 ± 0.24	31.23 ± 0.41	1.76 ± 0.06	5.09 ± 0.34	10.62 ± 0.16	4.34 ± 0.06
	40	30.74 ± 0.31	4.08 ± 0.02	0.72 ± 0.18	38.77 ± 0.26	2.27 ± 0.02	3.90 ± 0.21	9.95 ± 0.09	4.10 ± 0.01
	50	34.18 ± 0.26	5.07 ± 0.06	0.57 ± 0.09	42.18 ± 0.31	3.18 ± 0.05	3.50 ± 0.16	8.84 ± 0.14	3.89 ± 0.05
MRF	20	30.18 ± 0.12	3.51 ± 0.02	3.47 ± 0.21	30.44 ± 0.26	1.67 ± 0.03	7.07 ± 0.34	Not break	6.01 ± 0.03
	30	33.82 ± 0.18	4.05 ± 0.03	1.31 ± 0.12	37.51 ± 0.19	2.00 ± 0.03	5.62 ± 0.28	Not break	5.49 ± 0.03
	40	38.18 ± 0.21	4.88 ± 0.06	0.80 ± 0.09	42.44 ± 0.23	2.50 ± 0.06	4.08 ± 0.21	Not break	4.95 ± 0.06
	50	42.54 ± 0.35	5.77 ± 0.08	0.68 ± 0.07	48.02 ± 0.35	3.04 ± 0.05	3.46 ± 0.12	Not break	4.77 ± 0.04
TMRF	20	31.61 ± 0.28	3.61 ± 0.04	3.33 ± 0.11	32.27 ± 0.33	1.73 ± 0.04	6.94 ± 0.31	Not break	6.08 ± 0.04
	30	35.57 ± 0.11	4.15 ± 0.03	1.11 ± 0.16	38.87 ± 0.46	2.10 ± 0.03	5.56 ± 0.27	Not break	5.69 ± 0.07
	40	38.79 ± 0.39	5.03 ± 0.01	0.76 ± 0.09	43.83 ± 0.26	2.64 ± 0.02	3.98 ± 0.22	Not break	5.37 ± 0.06
	50	43.77 ± 0.27	5.89 ± 0.05	0.61 ± 0.12	48.54 ± 0.33	3.18 ± 0.05	3.32 ± 0.09	Not break	5.12 ± 0.02

In the same way, the stiffening of the material also implied a notable decrease in the elongation at break of the material. In all three cases, the elongation at break is significantly decreased by the incorporation of fibers and increased with increasing fiber content.

The better compatibility of the thermomechanical rapeseed fibers with BioPE is also visible in the bending test. The flexural strength results of the three-point bending specimens are shown in Table 3.

In this case, as for tensile strength, the use of fibers with a higher aspect ratio (TMRF) led to the greatest increases in flexural strength. In addition, the reinforcing effect produced by the fibers was also increased by incorporating a higher amount of rapeseed fibers, obtaining, with 50 wt.% rapeseed, increases for the BioPE matrix of 98.5, 125.9, and 128.4% for the composites with MR, MRF, and TMRF, respectively. It is worth noting that the trends in the same kind of composites are almost equal. This means the coupling agent has no effect on the flexural modulus; only the fiber content increases it in ratio.

To compare the impact properties of composite materials with unfilled matrix in the Charpy test, only notched specimens can be used since bio-polyethylene is a material with high impact strength and flexibility. It is also noteworthy that the only materials for which an impact resistance was obtained in the Charpy test without notching were the composites with MR, even with only 20 wt.%. Therefore, it is clear that the use of milled rapeseed results in a significant loss of impact resistance. In contrast, when fibers obtained by mechanical processing (MRF) and thermomechanical processing (TMRF) were used, this decrease was much smaller. In the notched samples, it was observed that the impact strength decreased with increasing fiber content. This effect is expected due to the greater brittleness of the material [41,42].

The evaluation of two different cases is presented below with the results obtained. The first case (Figure 6a) is the evaluation of the theoretical weight of the piece previously proposed (10 cm × 10 cm × 0.5 cm), modifying the thickness of the piece to obtain the same tensile strength of the original BioPE with the different composites. The second case (Figure 6b) is the theoretical tensile strength of the piece if it is intended to obtain a piece with a weight equal to that of the original piece, with the different composites produced.

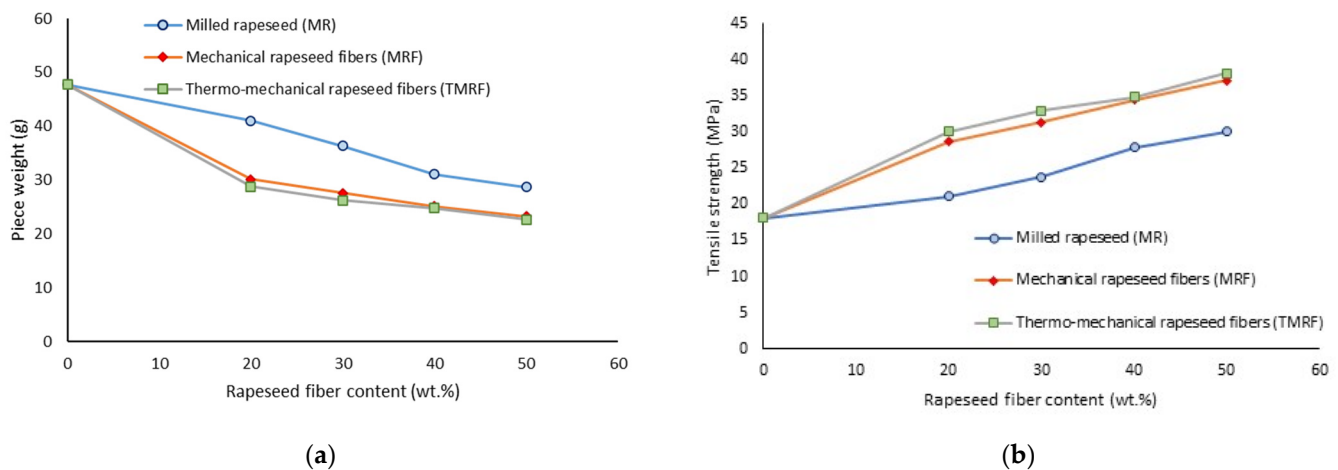


Figure 6. Evaluation of two different cases on plastic piece production: (a) piece with the same strength as the original BioPE; (b) piece with a weight equal to the original BioPE.

As can be seen in Figure 6a, the reinforcing capacity of the mechanical and thermomechanical fibers (MRF and TMRF) allows for further weight reduction. Likewise, a higher fiber content, even though it modifies the density of the material to a greater extent, leads to an increase in tensile strength, which counteracts this effect. Therefore, the higher the fiber content, the greater the ability to reduce the thickness of the piece and therefore its weight. In the most favorable case (50 wt.% TMRF), the thickness could be reduced from 5 cm to 2.07 cm, provided that the application where the part will be used allows it. Furthermore,

this reduction in the weight of the part, together with the presence of 50 wt.% of natural fibers, allows us to produce a part with the same mechanical properties yet with only 11.35 g of BioPE compared to the initial 47.75g (76.2% less).

Figure 6b shows how reducing the thickness of the part to control the weight increase results, in all cases, in tensile strengths higher than those of BioPE. Again, the most favorable case is with a 50 wt.% TMRF, which achieves a 110% increase in tensile strength with a part of equal weight (47.75 g) and a thickness of 0.44 cm. The manufacture of this part would imply consumption of 23.88 g of BioPE compared to 47.75 g of the initial part (50% less).

The results shown in both cases indicate that the production of these composite materials not only allows the integral use of agricultural waste, but also a more sustainable re-design of the semi-structural plastic components.

3.5. Composite Micromechanical Analysis

As discussed in Section 3.4, the tensile strength of composites with different rapeseed fibers progresses linearly as a function of the amount of reinforcement. This behavior allows the application of linear models for the study of micromechanics. In this case, the model known as the modified rule of mixtures (Equation (2)) was used:

$$\sigma_t^C = f_c \cdot \sigma_t^F \cdot V^F + (1 - V^F) \cdot \sigma_t^{m*}, \quad (2)$$

where σ_t^C is the maximum strength of the composite material, σ_t^F is the intrinsic fiber strength, σ_t^{m*} is the matrix strength at the point of maximum deformation of the composite material, and f_c is the efficiency factor. The latter is the product of two factors ($f_c = \chi_1 \cdot \chi_2$); the first factor (χ_1) takes into account the loss of properties due to fiber orientation in the composite and the second factor (χ_2) takes into account the interface between fiber and matrix and the length of the fibers.

χ_2 is calculated through the critical length, also known as the minimum fiber length to fully load a fiber according to the shear lag model [43] (Equation (3)).

$$L_c^F = \frac{d^F \cdot \sigma_t^F}{2 \cdot \tau}, \quad (3)$$

where d^F is the fiber diameter and τ is the interfacial tension.

The development of this model by Kelly and Tyson resulted in Equation (4) [44]. This expression reformulated from the rule of mixtures separates the contribution of fibers into two types of fibers according to their lengths: supercritical and subcritical. On the other hand, the orientation factor must be incorporated into the expression due to the non-orientation of all the fibers in the same direction.

$$\sigma_t^C = \chi_1 \cdot \left(\sum_{i=0}^{i=L_c} \left[\frac{\tau \cdot l_i^F \cdot V_i^F}{d^F} \right] + \sum_{j=L_c}^{j=\infty} \left[\sigma_t^F \cdot V_j^F \cdot \left(1 - \frac{\sigma_t^F \cdot d^F}{4 \cdot \tau \cdot l_j^F} \right) \right] \right) + (1 - V^F) \cdot \sigma_t^{m*}. \quad (4)$$

The Kelly and Tyson model presents four unknowns: χ_1 , τ , σ_t^F , and L_c^F , which can be solved using the method proposed by Bowyer and Bader. Bowyer and Bader considered that the intrinsic tensile strength of fibers can be approximated by the product of fibers intrinsic Young's modulus and elongation at the break of composite [45]. The intrinsic Young's modulus of the fiber can be determined using the Hirsch model [46]; therefore, an approximate value of the intrinsic tensile strength is obtained. The contributions of the subcritical fibers, supercritical length fibers, and the matrix can be expressed as X, Y, and Z, respectively. Therefore, Equations (2) and (3) can be rewritten as

$$\sigma_t^C = \chi_1 \cdot (X + Y) + Z. \quad (5)$$

To determine the contribution of subcritical and supercritical fibers, the fiber length distributions obtained for each of the composites were used, as shown in Figure 7.

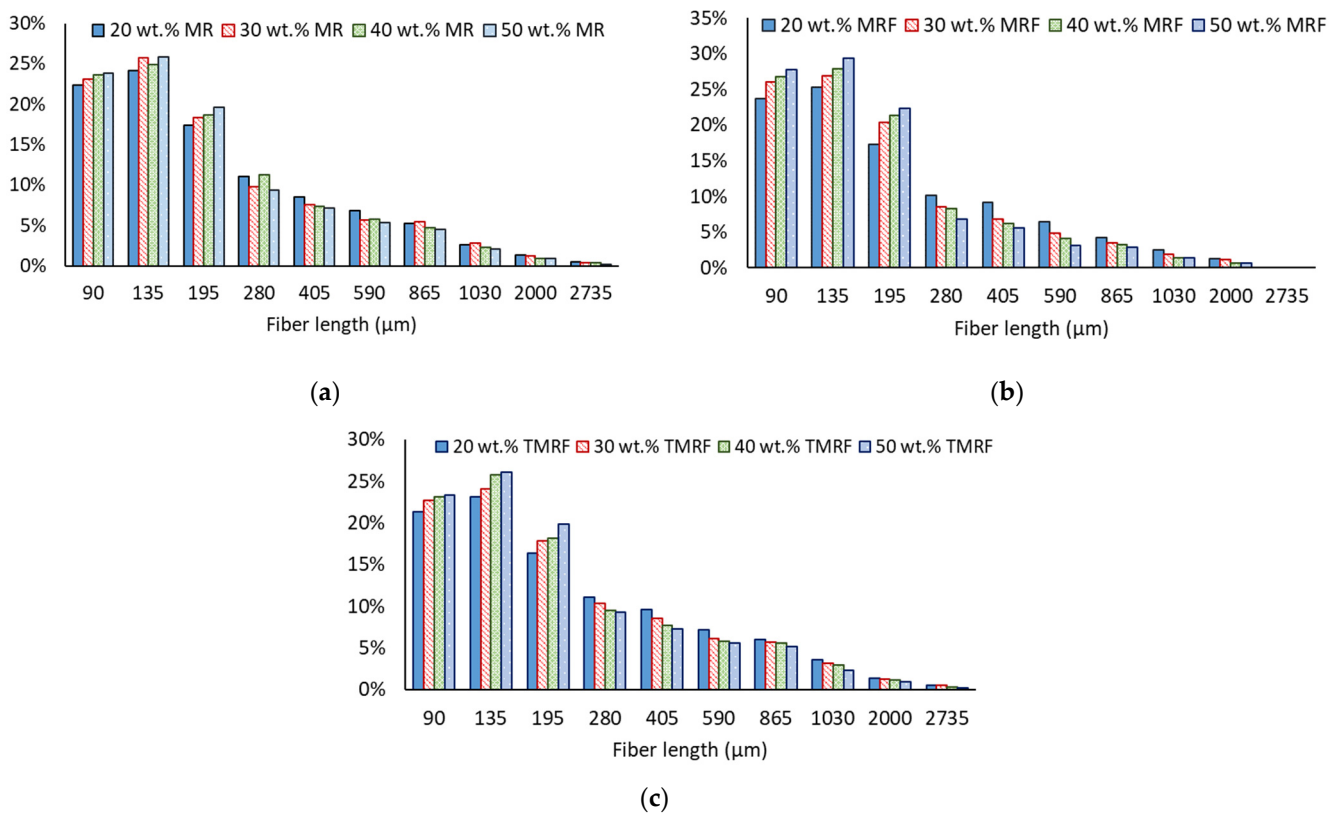


Figure 7. Fiber length distribution of (a) MR composites extracted fibers, (b) MRF composites extracted fibers, and (c) TMRF composites extracted fibers.

As shown, in all cases the highest percentage by weight of fibers is in the lower range of the scale. This leads us to believe that there will be a large percentage of fibers shorter than the critical length (subcritical fibers). Therefore, it is to be expected that a high percentage of fibers do not contribute substantially to the reinforcement of the material. Furthermore, it can be observed that an increase in the fiber content of the composite causes a further increase in this tendency, results that are in agreement with those presented in the literature [47,48]. However, micromechanical analysis is necessary to determine the contribution of the subcritical and supercritical fibers to the composite strength.

Bowyer and Bader's method of resolution requires the selection of two stress values (σ_1 and σ_2) and their respective strains (ε_1 and ε_2). This methodology requires the use of tensile strain curve characteristics for each composite (Figure 8).

In all composites, the values corresponding to 1/3 and 2/3 of the deformation at rupture of the composite were established. Through the elastic modulus of the matrix, the contribution of the matrix (Z) is calculated as the resistance that it is capable of exerting to the elongation at break of the composite. Once the matrix contribution is known, it is used to calculate R , as shown in Equation (6):

$$R = \frac{\sigma_1 - Z_1}{\sigma_2 - Z_2} = R^* = \frac{X_1 + Y_1}{X_2 + Y_2}. \quad (6)$$

On the other hand, a proposed value of τ is used to calculate the ratio R^* (theoretical). By adjusting the value until R and R^* are equal, it is possible to obtain the value of χ_1 through the Kelly and Tyson equation. This value must be equal to the two strain values used for each stress versus elongation at the break curve (Figure 8).

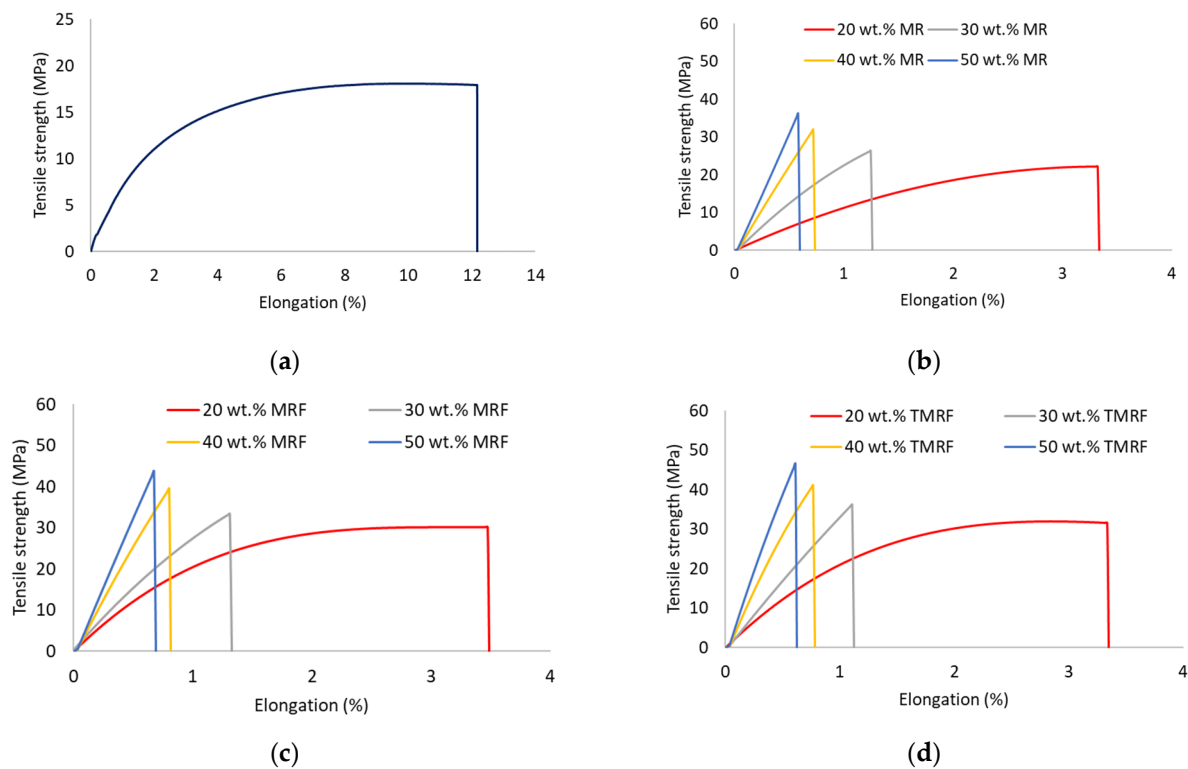


Figure 8. Tensile strength versus elongation at break for (a) bio-polyethylene, (b) MR-reinforced composites, (c) MRF-reinforced composites, and (d) TMRF-reinforced composites.

Once the parameters χ_1 and τ that allow solving the Kelly and Tyson equation have been obtained, it is possible to estimate the intrinsic resistance of the fibers by applying these values to Equation (3). Further, Equation (2) provides the coupling factor (f_c) value, which, as mentioned above, is the product of χ_1 and χ_2 . Finally, the orientation factor gives the mean orientation angle (α) as the average orientation angle ($\chi_1 = \cos^4 \alpha$).

Table 4 presents the results obtained from solving the Kelly and Tyson model for each of the different composites produced with MR, MRF, and TMRF rapeseed fibers.

Table 4. Micromechanical results of rapeseed-reinforced BioPE composites.

Fiber	Content (wt.%)	τ (MPa)	L_C (μm)	σ_t^F (MPa)	χ_1	χ_2	f_c	α ($^\circ$)
MR	20	9.73	565.51	371.68	0.27	0.66	0.18	61.19
	30	10.10	685.01	472.38	0.29	0.60	0.17	60.98
	40	10.26	702.24	493.65	0.29	0.57	0.17	60.90
	50	10.00	598.61	414.36	0.31	0.59	0.18	60.74
MRF	20	9.78	716.40	677.05	0.32	0.55	0.18	60.57
	30	9.76	708.37	688.27	0.33	0.53	0.17	60.49
	40	10.41	544.84	576.07	0.34	0.55	0.19	60.31
	50	9.99	563.73	577.50	0.32	0.52	0.17	60.58
TMRF	20	9.44	786.07	746.08	0.30	0.59	0.18	60.81
	30	9.18	814.69	759.49	0.30	0.57	0.17	60.83
	40	9.73	627.15	629.25	0.29	0.62	0.18	60.99
	50	9.42	587.12	573.34	0.29	0.60	0.17	60.95

It has been widely reported that for an interface to be considered strong, the value of the interfacial tension must be between the Tresca and von Mises criteria. In this sense, according to the Tresca criteria, the interfacial tension should be similar to $\tau = \sigma_t^M/2$, which

for BioPE would have a value of 9.06 MPa. While if the von Mises criterion ($\tau = \sigma_i^M / \sqrt{3}$) is taken into consideration, the value of the interfacial tension should be slightly higher, at 10.46 MPa [49,50]. In all cases, for the different methodologies used to obtain rapeseed fibers, τ values between 9.06 and 10.46 MPa are obtained. This does not mean that these fibers have a higher binding capacity with bio-polyethylene, but it shows that the use of 6% MAPE as a coupling agent allows for an increase in the interfacial interactions and therefore the interfacial shear strength.

On the other hand, the critical length value confirms in all cases a greater presence of subcritical fibers. This high critical length places the percentage of supercritical fibers, fibers with the highest contribution to tensile strength, at around 25%. These results, combined with the calculated intrinsic strength of the fibers, indicate that the supercritical fibers, even if they are found in a lower percentage, contribute significantly to the reinforcement of the material. This behavior has been widely reported in the literature when natural fibers are used for the reinforcement of plastic polymers [48]. The average σ_i^F values for MR, MRF, and TMRF composites are 637.8, 633.3, and 703.8 MPa respectively, in concordance with the literature [51,52].

Orientation factors are usually taken as reference values. It is known that the orientation of the fibers inside the composite material depends mainly on the characteristics of the injection molding machine used, mold geometry, and injection channels, as well as on the process parameters used. Therefore, a range of values for typical orientation factors is usually known for each equipment. In this case, orientation factors are known to be between 0.25 and 0.35 [48,53,54]. As shown in Table 4, in all cases the orientation factor obtained is in this range. The orientation factor values therefore allow us to validate the results obtained for the micromechanics of the compounds.

On the other hand, by using Equation (2) to determine the value of the intrinsic resistance of the fibers, the coupling factor can be obtained. In this case, the coupling factors are between 0.17 and 0.19, giving an average value of 0.18. This value is in the range (0.18–0.20) of optimum values for semi-aligned composites. As the coupling factor is the result of multiplying χ_1 by χ_2 , the values of the interface and length factor (χ_2) were determined. From the orientation factors obtained, the mean fiber orientation angle can be defined by the above-mentioned relationship. Then, it can be observed how the average orientation angle is in all cases close to 61°.

It can be concluded that in all cases a strong interface has been achieved and that the higher reinforcing capacity of TMRF fibers is mainly due to their morphology.

4. Conclusions

In the present work, we have demonstrated the feasibility of using agricultural waste as reinforcement of plastic materials with zero waste generation. Three different methods—milling, mechanical process, and thermomechanical process—have been validated as effective methods to obtain reinforcements. The influence of these treatments on the morphology of the fibers and the positive influence of the addition of a coupling agent has been verified. This has been optimized and the addition of this coupling agent at 6 wt.% obtained the maximum tensile strength. By studying the physical properties of the different composite materials, it was found that the influence of the treatment on the density of the fiber, as well as in the resulting composite, is superior in the case of the fibers obtained by thermomechanical treatment, with a higher aspect ratio. Through the study of Young's modulus and melt flow rate, a correct dispersion of the fibers in the material was determined. In addition, the greater difficulty of processing the milled rapeseed was observed when the fiber content was increased.

The addition of 20 to 50 wt.% rapeseed fibers with 6 wt.% ASM produces a linear increase in tensile strength and Young's modulus. Similarly, the flexural properties also increased. Remarkably, MRF and TMRF fibers have little influence on the impact strength, while MR fibers have a significant detrimental effect on this property. The study of the redesign of a part made with these materials showed it was possible to reduce the amount

of plastic polymer used by 76.2% with a 50 wt.% composite of TMRF fibers to obtain the same properties; alternately, a reduction of 50% is possible if the weight of the part is to be maintained, and the tensile strength of the final part is 110% higher than the initial value.

Finally, by studying the micromechanics of the composites, it was determined that the materials produced present a strong interface, as well as a typical orientation factor. In addition, it was found that the intrinsic strength of the fibers obtained by these sustainable methodologies was similar to typical values of natural fibers used as reinforcements.

Author Contributions: Investigation—methodology, R.A. and F.V.; data curation—review, F.X.E.; conceptualization—original draft preparation, Q.T.; writing—review and editing, M.D.-A.; supervision—project administration, P.M. All authors have read and agreed to the published version of the manuscript.

Funding: This research received no external funding.

Institutional Review Board Statement: Not applicable.

Informed Consent Statement: Not applicable.

Data Availability Statement: Not applicable.

Acknowledgments: Marc Delgado-Aguilar and Quim Tarrés are Serra Húnter Fellows.

Conflicts of Interest: The authors declare that they have no known competing financial interests or personal relationships that could have appeared to influence the work reported in this paper.

References

1. Gareiou, Z.; Chroni, C.; Kontoleon, K.; El Bachawati, M.; Saba, M.; Martin, R.H.; Zervas, E. Awareness of Citizens for the Single-Use Plastics: Comparison between a High-Income and an Upper-Middle-Income Economy of the Easter Mediterranean Region, Greece and Lebanon. *Sustainability* **2022**, *14*, 1912. [[CrossRef](#)]
2. Herberz, T.; Barlow, C.Y.; Finkbeiner, M. Sustainability assessment of a single-use plastics ban. *Sustainability* **2020**, *12*, 3746. [[CrossRef](#)]
3. Otoni, C.G.; Azeredo, H.M.C.; Mattos, B.D.; Beaumont, M.; Correa, D.S.; Rojas, O.J. The Food–Materials Nexus: Next Generation Bioplastics and Advanced Materials from Agri-Food Residues. *Adv. Mater.* **2021**, *33*, 2102520. [[CrossRef](#)] [[PubMed](#)]
4. Melchor-Martínez, E.M.; Macías-Garbett, R.; Alvarado-Ramírez, L.; Araújo, R.G.; Sosa-Hernández, J.E.; Ramírez-Gamboa, D.; Parra-Arroyo, L.; Alvarez, A.G.; Monteverde, R.P.B.; Cazares, K.A.S.; et al. Towards a Circular Economy of Plastics: An Evaluation of the Systematic Transition to a New Generation of Bioplastics. *Polymers* **2022**, *14*, 1203. [[CrossRef](#)]
5. Van den Oever, M.; Molenveld, K.; van der Zee, M.; Bos, H. *Bio-Based and Biodegradable Plastics: Facts and Figures*; Wageningen Food & Biobased Research: Wageningen, The Netherlands, 2017; ISBN 978-94-6343-121-7.
6. Bortolatto, R.; Bittencourt, P.R.S.; Yamashita, F. Biodegradable composites of starch/polyvinyl alcohol/soybean hull (*Glycine max* L.) produced by thermoplastic injection. *J. Appl. Polym. Sci.* **2022**, *139*, 52288. [[CrossRef](#)]
7. Lekrine, A.; Belaadi, A.; Makhoulouf, A.; Amroune, S.; Bourchak, M.; Satha, H.; Jawaid, M. Structural, thermal, mechanical and physical properties of Washingtonia filifera Fibres Reinforced Thermoplastic Biocomposites. *Mater. Today Commun.* **2022**, *31*, 103574. [[CrossRef](#)]
8. Fourati, Y.; Tarrés, Q.; Mutjé, P.; Boufi, S. PBAT/thermoplastic starch blends: Effect of compatibilizers on the rheological, mechanical and morphological properties. *Carbohydr. Polym.* **2018**, *199*, 51–57. [[CrossRef](#)]
9. Kiliç, E.; Tarrés, Q.; Delgado-Aguilar, M.; Espinach, X.; Fullana-I-palmer, P.; Puig, R. Leather waste to enhance mechanical performance of high-density polyethylene. *Polymers* **2020**, *12*, 2016. [[CrossRef](#)]
10. Brodin, M.; Vallejos, M.; Opedal, M.T.; Area, M.C.; Chinga-Carrasco, G. Lignocellulosics as sustainable resources for production of bioplastics—A review. *J. Clean. Prod.* **2017**, *162*, 646–664. [[CrossRef](#)]
11. Ferrero, B.; Fombuena, V.; Fenollar, O.; Boronat, T.; Balart, R. Development of Natural Fiber-Reinforced Plastics (NFRP) Based on Biobased Polyethylene and Waste Fibers From *Posidonia oceanica* Seaweed. *Polym. Polym. Compos.* **2008**, *36*, 1378–1385. [[CrossRef](#)]
12. Shah, N.; Fehrenbach, J.; Ulven, C.A. Hybridization of hemp fiber and recycled-carbon fiber in polypropylene composites. *Sustainability* **2019**, *11*, 3163. [[CrossRef](#)]
13. Reixach, R.; Espinach, F.X.; Arbat, G.; Julián, F.; Delgado-Aguilar, M.; Puig, J.; Mutjé, P. Tensile properties of polypropylene composites reinforced with mechanical, thermomechanical, and chemi-thermomechanical pulps from orange pruning. *BioResources* **2015**, *10*, 4544–4556. [[CrossRef](#)]
14. Serra, A.; Tarrés, Q.; Llop, M.; Reixach, R.; Mutjé, P.; Espinach, F.X. Recycling dyed cotton textile byproduct fibers as polypropylene reinforcement. *Text. Res. J.* **2019**, *89*, 2113–2125. [[CrossRef](#)]

15. Pickering, K.L.; Efendy, M.G.A.; Le, T.M. A review of recent developments in natural fibre composites and their mechanical performance. *Compos. Part A Appl. Sci. Manuf.* **2016**, *83*, 98–112. [[CrossRef](#)]
16. Yang, H.S.; Wolcott, M.P.; Kim, H.S.; Kim, H.J. Thermal properties of lignocellulosic filler-thermoplastic polymer bio-composites. *J. Therm. Anal. Calorim.* **2005**, *82*, 157–160. [[CrossRef](#)]
17. Deng, Y.; Tian, Y. Assessing the environmental impact of flax fibre reinforced polymer composite from a consequential life cycle assessment perspective. *Sustainability* **2015**, *7*, 11462–11483. [[CrossRef](#)]
18. Rajput, P.; Sarin, M.; Sharma, D.; Singh, D. Characteristics and emission budget of carbonaceous species from post-harvest agricultural-waste burning in source region of the Indo-Gangetic plain. *Tellus Ser. B Chem. Phys. Meteorol.* **2014**, *66*, 21026. [[CrossRef](#)]
19. Jannat, A.; Ishikawa-ishiawata, Y. Does Climate Change Affect Rapeseed Production in Exporting and Importing Countries? Evidence from Market Dynamics Syntheses. *Sustainability* **2022**, *14*, 6051. [[CrossRef](#)]
20. D’Odorico, P.; Davis, K.F.; Rosa, L.; Carr, J.A.; Chiarelli, D.; Dell’Angelo, J.; Gephart, J.; MacDonald, G.K.; Seekell, D.A.; Suweis, S.; et al. The Global Food-Energy-Water Nexus. *Rev. Geophys.* **2018**, *56*, 456–531. [[CrossRef](#)]
21. Jiang, S.; Li, B.; Shen, Y. The influence of pulp and paper industry on environment. *Web Conf.* **2021**, *308*, 02007. [[CrossRef](#)]
22. Anastas, P.; Warner, J. *Green Chemistry: Theory and Practice*; Oxford University Press: Oxford, UK, 1998.
23. Mboowa, D. A review of the traditional pulping methods and the recent improvements in the pulping processes. *Biomass Convers. Biorefin.* **2021**, *1*, 1–12. [[CrossRef](#)]
24. Biermann, C. *Handbook of Pulping and Papermaking*, 2nd ed.; Elsevier: Amsterdam, The Netherlands, 1996; ISBN 9780120973620.
25. Das, T.K.; Houtman, C. Evaluating chemical-, Mechanical-, and bio-pulping processes and their sustainability characterization using life-cycle assessment. *Environ. Prog.* **2004**, *23*, 347–357. [[CrossRef](#)]
26. Li, Y. Effect of coupling agent concentration, fiber content, and size on mechanical properties of wood/HDPE composites. *Int. J. Polym. Mater. Polym. Biomater.* **2012**, *61*, 882–890. [[CrossRef](#)]
27. El-Sabbagh, A. Effect of coupling agent on natural fibre in natural fibre/polypropylene composites on mechanical and thermal behaviour. *Compos. Part B Eng.* **2014**, *57*, 126–135. [[CrossRef](#)]
28. Kakou, C.A.; Arrakhiz, F.Z.; Trokourey, A.; Bouhfid, R.; Qaiss, A.; Rodrigue, D. Influence of coupling agent content on the properties of high density polyethylene composites reinforced with oil palm fibers. *Mater. Des.* **2014**, *63*, 641–649. [[CrossRef](#)]
29. Rao, J.; Zhou, Y.; Fan, M. Revealing the interface structure and bonding mechanism of coupling agent treated WPC. *Polymers* **2018**, *10*, 266. [[CrossRef](#)]
30. Karimah, A.; Ridho, M.R.; Munawar, S.S.; Adi, D.S.; Ismadi; Damayanti, R.; Subiyanto, B.; Fatriasari, W.; Fudholi, A. A review on natural fibers for development of eco-friendly bio-composite: Characteristics, and utilizations. *J. Mater. Res. Technol.* **2021**, *13*, 2442–2458. [[CrossRef](#)]
31. Stark, N.M.; Matuana, L.M.; Clemons, C.M. Effect of processing method on surface and weathering characteristics of wood-flour/HDPE composites. *J. Appl. Polym. Sci.* **2004**, *93*, 1021–1030. [[CrossRef](#)]
32. Teuber, L.; Militz, H.; Krause, A. Processing of wood plastic composites: The influence of feeding method and polymer melt flow rate on particle degradation. *J. Appl. Polym. Sci.* **2016**, *133*, 43231. [[CrossRef](#)]
33. Anand Raj, M.K.; Muthusamy, S.; Panchal, H.; Mahmoud Ibrahim, A.M.; Alsoufi, M.S.; Elsheikh, A.H. Investigation of mechanical properties of dual-fiber reinforcement in polymer composite. *J. Mater. Res. Technol.* **2022**, *18*, 3908–3915. [[CrossRef](#)]
34. Haque, M.E.; Khan, M.W.; Rani, M. Studies on morphological, physico-chemical and mechanical properties of wheat straw reinforced polyester resin composite. *Polym. Bull.* **2022**, *79*, 2933–2952. [[CrossRef](#)]
35. Thabab, W.; Kumar Singh, A.; Bedi, R. Tensile properties of urea treated rice straw reinforced recycled polyethylene terephthalate composite materials. *Mater. Today Proc.* **2022**, *56*, 2151–2157. [[CrossRef](#)]
36. Kusić, D.; Božič, U.; Monzón, M.; Paz, R.; Bordón, P. Thermal and Mechanical Characterization of Banana Fiber Reinforced Composites for Its Application in Injection Molding. *Materials* **2020**, *13*, 3581. [[CrossRef](#)] [[PubMed](#)]
37. Ehman, N.V.; Ita-Nagy, D.; Felissia, F.E.; Vallejos, M.E.; Quispe, I.; Area, M.C.; Chinga-Carrasco, G. Hydrothermal-Alkaline Sugarcane Bagasse Pulp and Coupled with a Bio-Based Compatibilizer. *Molecules* **2020**, *25*, 2158. [[CrossRef](#)] [[PubMed](#)]
38. Ahmad, F.; Choi, H.S.; Park, M.K. A review: Natural fiber composites selection in view of mechanical, light weight, and economic properties. *Macromol. Mater. Eng.* **2015**, *300*, 10–24. [[CrossRef](#)]
39. Mulinari, D.R.; Voorwald, H.J.C.; Cioffi, M.O.H.; da Silva, M.L.C.P.; da Cruz, T.G.; Saron, C. Sugarcane bagasse cellulose/HDPE composites obtained by extrusion. *Compos. Sci. Technol.* **2009**, *69*, 214–219. [[CrossRef](#)]
40. Tarrés, Q.; Hernández-díaz, D.; Ardanuy, M. Interface strength and fiber content influence on corn stover fibers reinforced bio-polyethylene composites stiffness. *Polymers* **2021**, *13*, 768. [[CrossRef](#)]
41. López, J.P.; Gironès, J.; Mendez, J.A.; Pèlach, M.A.; Vilaseca, F.; Mutjé, P. Impact and flexural properties of stone-ground wood pulp-reinforced polypropylene composites. *Polym. Compos.* **2013**, *34*, 842–848. [[CrossRef](#)]
42. Oliver-Ortega, H.; Tarrés, Q.; Mutjé, P.; Delgado-Aguilar, M.; Méndez, J.A.; Espinach, F.X. Impact strength and water uptake behavior of bleached kraft softwood-reinforced PLA composites as alternative to PP-based materials. *Polymers* **2020**, *12*, 2144. [[CrossRef](#)]
43. Tucker, C.L.; Liang, E. Stiffness predictions for unidirectional short-fiber composites: Review and evaluation. *Compos. Sci. Technol.* **1999**, *59*, 655–671. [[CrossRef](#)]

44. Kelly, A.; Tyson, W. Tensile properties of fibre-reinforced metals-copper/tungsten and copper/molybdenum. *J. Mech. Phys. Solids* **1965**, *13*, 329–338. [[CrossRef](#)]
45. Bowyer, W.H.; Bader, H.G. On the reinforcement of thermoplastics by imperfectly aligned discontinuous fibres. *J. Mater. Sci.* **1972**, *7*, 1315–1321. [[CrossRef](#)]
46. Hirsch, T.J. Modulus of Elasticity of Concrete Affected by Elastic Moduli of Cement Paste Matrix and Aggregate. *J. Proc.* **1962**, *59*, 427–452.
47. Salem, S.; Oliver-ortega, H.; Espinach, F.X.; Hamed, K.B.; Nasri, N.; Alcalà, M.; Mutjé, P. Study on the Tensile Strength and Micromechanical Analysis of Alfa Fibers Reinforced High Density Polyethylene Composites. *Fibers Polym.* **2019**, *20*, 602–610. [[CrossRef](#)]
48. Serrano, A.; Espinach, F.X.; Julian, F.; Del Rey, R.; Mendez, J.A.; Mutje, P. Estimation of the interfacial shears strength, orientation factor and mean equivalent intrinsic tensile strength in old newspaper fiber/polypropylene composites. *Compos. Part B Eng.* **2013**, *50*, 232–238. [[CrossRef](#)]
49. Thomason, J.L. Interfacial strength in thermoplastic composites—At last an industry friendly measurement method? *Compos. Part A Appl. Sci. Manuf.* **2002**, *33*, 1283–1288. [[CrossRef](#)]
50. Pegoretti, A.; Della Volpe, C.; Detassis, M.; Migliaresi, C.; Wagner, H.D. Thermomechanical behaviour of interfacial region in carbon fibre/epoxy composites. *Compos. Part A Appl. Sci. Manuf.* **1996**, *27*, 1067–1074. [[CrossRef](#)]
51. Kompella, M.K.; Lambros, J. Micromechanical characterization of cellulose fibers. *Polym. Test.* **2002**, *21*, 523–530. [[CrossRef](#)]
52. Bledzki, A.K.; Gassan, J. Composites reinforced with cellulose_Bledzki_1999.pdf. *Prog. Polym. Sci.* **1999**, *24*, 221–274. [[CrossRef](#)]
53. Espinach, F.X.; Granda, L.A.; Tarrés, Q.; Duran, J.; Fullana-I-Palmer, P.; Mutjé, P. Mechanical and micromechanical tensile strength of eucalyptus bleached fibers reinforced polyoxymethylene composites. *Compos. Part B Eng.* **2016**, *116*, 333–339. [[CrossRef](#)]
54. Oliver-Ortega, H.; Llop, M.F.; Espinach, F.X.; Tarrés, Q.; Ardanuy, M.; Mutjé, P. Study of the flexural modulus of lignocellulosic fibers reinforced bio-based polyamide11 green composites. *Compos. Part B Eng.* **2018**, *152*, 126–132. [[CrossRef](#)]